Original Article | Gastrointestinal Imaging

http://dx.doi.org/10.3348/kjr.2015.16.3.531
pISSN 1229-6929 · eISSN 2005-8330
Korean J Radiol 2015;16(3):531-540

Korean Journal of Radiology
KJR

Combined Use of Automatic Tube Voltage Selection and Current Modulation with Iterative Reconstruction for CT Evaluation of Small Hypervascular Hepatocellular Carcinomas: Effect on Lesion Conspicuity and Image Quality

Peijie Lv, MD[1], Jie Liu, MM[1], Rui Zhang, MM[1], Yan Jia, MD[2], Jianbo Gao, MD[1]

[1]Department of Radiology, The First Affiliated Hospital of Zhengzhou University, Zhengzhou, Henan Province 450052, China; [2]Siemens Healthcare China, Beijing 100102, China

Objective: To assess the lesion conspicuity and image quality in CT evaluation of small (≤ 3 cm) hepatocellular carcinomas (HCCs) using automatic tube voltage selection (ATVS) and automatic tube current modulation (ATCM) with or without iterative reconstruction.

Materials and Methods: One hundred and five patients with 123 HCC lesions were included. Fifty-seven patients were scanned using both ATVS and ATCM and images were reconstructed using either filtered back-projection (FBP) (group A1) or sinogram-affirmed iterative reconstruction (SAFIRE) (group A2). Forty-eight patients were imaged using only ATCM, with a fixed tube potential of 120 kVp and FBP reconstruction (group B). Quantitative parameters (image noise in Hounsfield unit and contrast-to-noise ratio of the aorta, the liver, and the hepatic tumors) and qualitative visual parameters (image noise, overall image quality, and lesion conspicuity as graded on a 5-point scale) were compared among the groups.

Results: Group A2 scanned with the automatically chosen 80 kVp and 100 kVp tube voltages ranked the best in lesion conspicuity and subjective and objective image quality (p values ranging from < 0.001 to 0.004) among the three groups, except for overall image quality between group A2 and group B (p = 0.022). Group A1 showed higher image noise (p = 0.005) but similar lesion conspicuity and overall image quality as compared with group B. The radiation dose in group A was 19% lower than that in group B (p = 0.022).

Conclusion: CT scanning with combined use of ATVS and ATCM and image reconstruction with SAFIRE algorithm provides higher lesion conspicuity and better image quality for evaluating small hepatic HCCs with radiation dose reduction.

Index terms: *Automatic tube voltage selection; Automatic tube current modulation; Sinogram-affirmed iterative reconstruction; Small hepatocellular carcinoma*

INTRODUCTION

There has been a rapid increase in the use of computed tomography (CT). The risks, such as radiation, and the benefits, such as good anatomic resolution, are hotly debated. Many studies have documented the radiation doses that patients receive from medical imaging, with particular attention devoted to CT (1-8). It is crucial to keep radiation doses as low as possible. Multidetector CT protocols can be optimized in a variety of ways to reduce the overall radiation dose, including automatic tube current modulation (ATCM), individualization of acquisition protocols by decreasing the number of scanning phases, adjustment of the tube peak voltage (kVp setting) and tube current-time product (milliampere-seconds, mAs), or use of noise

Received June 7, 2014; accepted after revision January 15, 2015.
Corresponding author: Jianbo Gao, MD, Department of Radiology, The First Affiliated Hospital of Zhengzhou University, No.1, East Jianshe Road, Zhengzhou, Henan Province 450052, China.
• Tel: (86371) 66913114-6809 • Fax: (86371) 66970906
• E-mail: jianbogao0307@163.com

reduction filters.

Automatic tube current modulation is the most frequently (9, 10) used method to reduce radiation dose, by adjusting tube current based on the size and attenuation characteristics of the body part being scanned, while X-ray tube voltage (kVp setting) is left unchanged. Optimization of tube voltage has great potential in radiation dose reduction (11-13). Automatic tube voltage selection (ATVS), which automatically recommends the optimal tube voltage setting for each patient and clinical indication, has been taken into account by the diagnostic task of the CT study (14-19). As a trade-off for the advantage of higher iodine attenuation at lower tube voltages, a slightly higher image noise and reduced overall image quality are accepted (17, 20). A sinogram-affirmed iterative reconstruction (SAFIRE) algorithm for CT image reconstruction is applicable in clinical practice and it can be used either to improve image quality at a constant radiation dose or to reduce radiation dose at a constant image quality (10, 21-23). The use of each of the two techniques has been repetitively demonstrated in various studies. The combination of automatic attenuation-based tube voltage selection and iterative reconstruction (IR) has been examined for coronary CT angiography (18), chest CT angiography (15), and CT examinations of the chest, abdomen, and pelvis (22, 24), and a liver phantom containing hypodense lesions (16). However, the CT protocol with combination of ATVS and current modulation and IR has not been thoroughly investigated for the evaluation of small hypervascular hepatocellular carcinomas (HCCs) in the prior studies.

Therefore, the purpose of our study was to assess the lesion conspicuity and image quality in CT evaluation of small (≤ 3 cm) HCCs using ATVS and ATCM with or without IR.

MATERIALS AND METHODS

This prospective study was approved by our Institutional Review Board and all patients provided written informed consent before participation in the study.

Patient Population

The ATVS protocol was applied for clinical liver CT imaging at our institution in January 2013. From January 2013 to March 2014, 212 consecutively registered patients with known or suspected primary hypervascular liver tumors on previous imaging studies or an abnormally increased liver tumor marker (alpha fetoprotein [AFP] > 11 ng/mL) level underwent CT imaging. Patients were considered ineligible if they were younger than 18 years of age, pregnant or lactating, or had any contraindication to iodinated contrast material. Patients who had reliable evidence of primary HCCs with size smaller than or equal to 3 cm in diameter were included. The clinical diagnostic reference standard of HCC was confirmed by means of histological findings after lobectomy or segmentectomy, and typical CT imaging investigations with high levels of serum AFP or with lipiodized oil (Lipiodol Ultra-fluid; Guerbet, Aulnay-sous-Bois, France) uptake at follow-up CT examinations performed at 4-week intervals after transcatheter arterial chemoembolization (25). The classic description of HCC includes a hypervascular lesion in the hepatic arterial phase with wash-out in the portal venous phase (PVP). Delayed-phase scan was not routinely performed at our institution due to radiation concerns. The number of lesions in one patient was less than or equal to 2. One hundred and seven (50.5%) of the 212 patients were excluded because 1) patients had multiple lesions (equal to or more than 3 lesions) (n = 13); 2) there was failure of each lesion to meet the clinical diagnostic reference standard (n = 43); 3) the largest diameter of each lesion was greater than 3 cm (n = 35); 4) there was a technical failure during contrast injection (n = 16).

One hundred and five patients (71 men and 34 women; mean age: 56 years, range: 23–81 years) with 123 HCC lesions (mean diameter 2.3 cm, 0.9–3.0 cm) confirmed by means of histological findings (n = 56), typical CT findings with high levels of serum AFP (n = 29) or with lipiodized oil uptake (n = 38) were included in our study. Among 80% of the lesions with typical imaging features in the entire patient population, 32 lesions were histologically confirmed. Patients were divided into two groups (A and B) on the basis of the study period and imaging protocol used. In the first half of the study period, 57 patients with 66 lesions underwent CT imaging using the combined ATVS and ATCM protocol (group A). In the remaining half of the study period, 48 patients with 57 lesions underwent CT imaging using the standard ATCM protocol with a fixed tube voltage of 120 kVp (group B).

Automatic Tube Voltage Selection

Automatic tube voltage selection software (Care kVp, Siemens Healthcare, Forchheim, Germany) is an intelligent optimal kVp scanning technology, which can automatically recommend tube voltage settings that provide the lowest

Korean Journal of Radiology
KJR

radiation dose and high image quality based on the patient's body size and diagnostic task (14, 17). The scan scheme is selected according to the diagnostic task, while the patient's body size is identified based on the topogram image. ATCM (CARE Dose 4D; Healthcare, Forchheim, Germany) then modulates the tube current for adjusting the radiation dose on the basis of user-specified image quality and X-ray attenuation characteristics of the scanned body region (26). Patient-specific tube current values for different tube voltages (80, 100, 120, and 140 kVp) are automatically calculated based on the patient's geometry and anatomy. Scan range and operator-selected contrast gain settings are selected for each type of CT examination (setting 1 indicates no contrast gain and setting 12 indicates a high level of contrast with respect to the desired image characteristics) (17). The estimated radiation doses for all of the tube voltage and current combinations are calculated and the optimal combination with the lowest radiation dose is selected. If a selected tube voltage setting is not possible because of tube hardware system limitations, e.g., exceeding the maximal tube current, the next best setting is selected.

Scanning Protocols and Contrast Injection

All patients underwent triple-phase CT imaging (precontrast, late arterial phase [LAP], PVP) on a second-generation dual-source CT (SOMATOM Definition Flash, Siemens Healthcare, Forchheim, Germany) in the standard single-energy CT mode. Fifty-seven patients in group A underwent CT scans using a combination of the ATVS (Care kVp) and ATCM (CARE Dose 4D) protocol for LAP and PVP. The pre-setting reference tube potential and reference tube current were 120 kVp and 210 mAs, respectively. The Care kVp setting was maintained on the "liver" position for all patients (7 out of 12 on the basis of the vendor's recommendations). Forty-eight patients in group B underwent CT imaging using the standard ATCM protocol with a fixed tube voltage of 120 kVp and the reference tube current of 300 mAs for all phases. Standard scanning parameters were collimation 64 x 0.6 mm, gantry rotation time 0.5 seconds, pitch 0.9, acquisition slice thickness 5 mm, and scanning field of view 50 cm.

A total of 60–100 mL (1.2 mL/kg) nonionic IV contrast material (iohexol [Omnipaque], 350 mg I/mL, GE Healthcare, Milwaukee, WI, USA) was injected at a rate of 3–4 mL/s with a power injector (Envision CT Injector, Medrad, GA, USA) through a 20-G catheter inserted into an antecubital vein. The start of image acquisition was automatically triggered 7 seconds after the predetermined threshold (100 Hounsfield unit [HU]) was reached in a region-of-interest placed at the level of the supraceliac abdominal aorta. Hepatic PVP imaging began 30 seconds after the LAP. Images of the hepatic venous phase were also acquired during a single breath-hold by helical scan of the liver using the same protocol as that for the LAP scan. These image sets were not included in the quantitative and qualitative analyses.

Images acquired using the combined ATVS and ATCM protocol were reconstructed by using the filtered back-projection (FBP) algorithm with a standard abdomen kernel (B30f) (group A1) or the SAFIRE (I30f) algorithm with filter strength 3 (group A2) (27). Images acquired using the ATCM protocol with a fixed tube voltage of 120 kVp were reconstructed by using the FBP algorithm (B30f) (group B). Images from all three groups were reconstructed at a slice thickness of 1 mm with an increment of 1 mm. All images were transferred to a postprocessing workstation (MultiModality Workplace, Siemens, Forchheim, Germany) for image evaluation.

Tube Voltage Selection and Body Mass Index Analysis

The patients were categorized into four groups according to their body mass indices (BMI) (less than 18.5 kg/m^2, underweight; between 18.5 and 23.9 kg/m^2, normal BMI; between 24 and 28.9 kg/m^2, overweight; and 29 kg/m^2 or greater, obese) (28). The recommended tube voltages were analyzed on the basis of the four BMI groups.

Image Analysis

Quantitative Analysis

A single reviewer with 5 years of experience in reading abdominal CT performed the quantitative analysis using a commercially available workstation (Siemens Multi Modality Workplace). The attenuation values (i.e., CT number in HU) of the hepatic lesions and the liver parenchyma adjacent to each lesion, the non-tumor liver, the abdominal aorta, and the para-spinal muscles were measured. Hypervascular liver lesions were assessed by manually placing circular or ovoid regions-of-interest (ROIs), which were drawn to encompass the hyperenhancing portion of the lesion as much as possible from three contiguous slices. Mean CT data for the adjacent hepatic parenchyma as the background regions were obtained by manually placing circular ROIs in the

hepatic parenchyma. The attenuation of the non-tumor liver was recorded as the mean measurement of three ROIs placed in the anterior and posterior segments of the right hepatic lobe and in the medial segments of the left hepatic lobe. Areas of focal changes in parenchymal density, large vessels and prominent artefacts, if any, were carefully avoided. The ROIs in the vessels were maintained as large as possible and care was taken to avoid calcifications and/or soft plaques. A quantitative marker of image noise in each group was defined as the standard deviation (SD_n) of the attenuation value (HU) in a homogeneous region of the subcutaneous fat on the anterior abdominal wall. Attenuation of the latissimus dorsi muscle (ROI_m), not including macroscopic areas of fat infiltration, was measured in the same image sets.

Contrast-to-noise ratio (CNR) relative to muscle for the organ of interest (non-tumor liver and aorta) was calculated by using the equation $CNR_{liver\ or\ aorta} = (ROI_{liver\ or\ aorta} - ROI_m) / SD_n$, where $ROI_{liver\ or\ aorta}$ was the mean attenuation of the liver or the aorta, ROI_m was the mean attenuation of the paraspinal muscle, and SD_n was the mean image noise. Lesion-to-liver contrast-to-noise ratios (CNR_{lesion}) were calculated as follows: $CNR_{lesion} = (ROI_{lesion} - ROI_{liver}) / SD_n$, where the ROI_{lesion} and ROI_{liver} were the mean attenuation of the lesion and the hepatic parenchyma adjacent to the tumor, respectively.

Qualitative Analysis

Two radiologists with 14–30 years of experience in reading abdominal CT independently performed a blinded qualitative analysis among the three groups of liver CT image sets during the LAP, using the same workstation. A total of 162 images for image noise and overall image quality, and 189 images for lesion conspicuity in groups A and B were evaluated. The images of each patient were presented in a random order to the readers. Readers were blinded to the CT scanning protocols as well as to patient demographics. Although the default display window width and level settings were initially presented (window width, 220 HU; window level, 40 HU), readers were allowed to modify the window width and level at their own discretion.

Image noise, overall image quality of the liver, and lesion conspicuity were evaluated. The grading of the image noise was also incorporated into the assessment of the overall image quality. A five-point subjective scale was used to grade image noise (1 = unacceptable; 2 = substantial, above average; 3 = moderate, average; 4 = minor, below average; 5 = absent) (29) and overall image quality (1 = unacceptable, no diagnosis possible; 2 = poor diagnostic value, just acceptable; 3 = moderate; 4 = good; 5 = excellent) (30). For analysis of lesion conspicuity (17, 31) the following five-point ordinal scale was used: score 5, definitely distinct; score 4, fairly distinct; score 3, moderately distinct; score 2, barely distinct; score 1, not distinct.

Radiation Dose Evaluation

Scan length (distance covered) was documented for groups A and B. The radiation dose in CT dose index (CTDIvol, mGy) for each examination was recorded from the CT system. The effective dose was calculated by multiplying the dose-length product (DLP, mGy·cm) by a conversion factor of 0.015 for abdominal examination (32).

Statistical Analysis

All statistical calculations were performed using SAS, version 9.1.3 (SAS, Cary, NC, USA). Continuous variables were reported as means and SD. Categorical variables were reported as frequencies or percentages. Age, BMI, mean size of lesions and effective dose were compared between groups A and B using the independent *t* test. Gender differences were evaluated using the Mann-Whitney U test. For image noise and CNR, a paired *t* test was used to compare between groups A1 and A2 while the Student's *t* test was used to compare between groups A (either 1 or 2) and B. For the results of qualitative analysis, the Wilcoxon signed rank test was used to compare between groups A1 and A2 while the Mann-Whitney U test was used to compare between groups A (either 1 or 2) and B. Spearman's rank correlation coefficient was calculated for the correlations between BMI and tube voltage. Interobserver agreement was calculated by using Cohen κ values. Significance criterion was overall alpha of 0.05. Therefore, for the pairwise comparisons among the three groups (A1, A2, and B), $p < 0.017$ was considered to be statistically significant, i.e., Bonferroni correction.

RESULTS

There was no significant difference between groups A and B in gender (M:F, 36:21 vs. 37:11, $p = 0.121$), age (53.3 ± 12.8 years vs. 54.3 ± 11.7 years, $p = 0.818$), BMI (24.1 ± 3.4 kg/m^2 vs. 24.3 ± 3.3 kg/m^2, $p = 0.747$) or mean size of evaluated lesions (19.9 ± 11.3 mm vs. 21.2 ± 20.8 mm, $p = 0.204$).

BMI Analysis

In group A, two (3.5%) patients had BMI values < 18.5

Korean Journal of Radiology
KJR

kg/m^2, 23 patients (40.4%) had BMI values between 18.5 and 23.9 kg/m^2, 27 patients (47.4%) had BMI values between 24 and 28.9 kg/m^2, and 5 patients (8.8%) had BMI values ≥ 29 kg/m^2. The correlation between BMI and recommended tube voltage was moderate (coefficient = 0.401, p = 0.002) (Fig. 1).

100 kVp was the most frequent automatically chosen tube voltage in all four BMI groups, accounting for 100% (2/2) in underweight patients, 74% (17/23) in patients with normal BMI, 89% (24/27) in overweight patients, and 60% (3/5) in obese patients, and there were 3, 18, 24, and 4 lesions in these four groups, respectively. A tube voltage of 80 kVp was used in 26% (6/23) of patients with normal BMI and in 7% (2/27) of overweight patients with 9 and 5 lesions, respectively. A tube voltage of 120 kVp was only used in one overweight patient (4%, 1/27) with one lesion, while a tube voltage of 140 kVp was only used in two obese patients (40%, 2/5) with 2 lesions. Considering the small number of patients, 120 kVp and 140 kVp were excluded from the kVp-specific analysis.

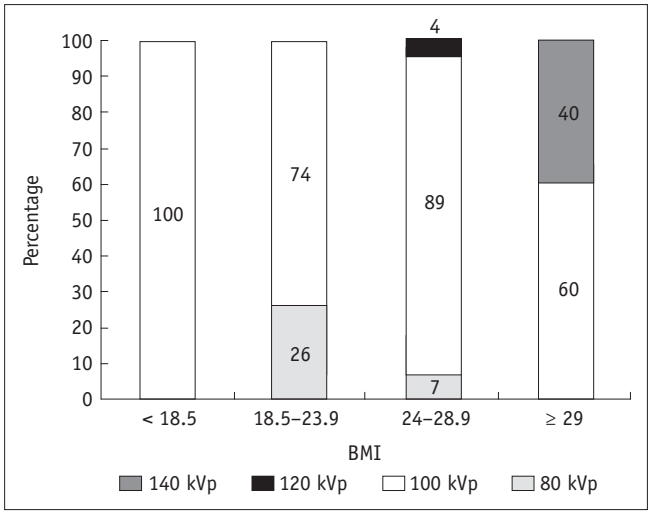

Fig. 1. Distribution of selected tube voltages in group A according to BMI. BMI = body mass indices

Quantitative Analysis

Contrast-to-noise ratio and image noise in the three groups are shown in Table 1 and Figure 2. There was no significant difference in liver attenuation among the three groups (p > 0.05). The CNRs of the aorta, all lesions, and lesions scanned with the chosen 80 kVp and 100 kVp tube voltage in group A2 were significantly higher than those in group A1 and group B (p values ranging from < 0.001 to

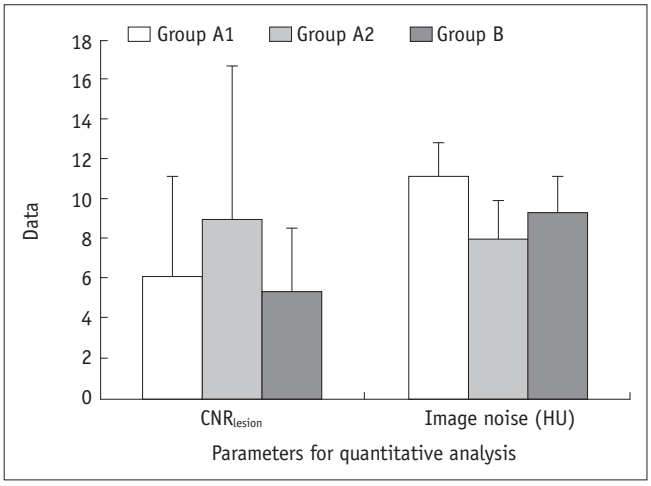

Fig. 2. Results of quantitative analysis for all lesions with respect to CNR_{lesion} and image noise among three groups. Among three groups, CNR_{lesion} was highest and image noise was lowest in group A2 (p values ranging from < 0.001 to 0.004). Compared with group B, CNR_{lesion} in group A1 was not significantly different (p > 0.05) while image noise in group A1 was significantly higher (p = 0.002). CNR = contrast-to-noise ratio, HU = Hounsfield unit

Table 1. Quantitative Analysis Results in 3 Groups

Parameter		Groups			*P*		
		Group A1 (57 Patients with 66 Lesions)	Group A2 (57 Patients with 66 Lesions)	Group B (48 Patients with 57 Lesions)	A1 vs. A2	A1 vs. B	A2 vs. B
CNR_{liver}	All	0.87 ± 0.55	1.03 ± 0.79	0.86 ± 0.68	0.048	0.935	0.261
CNR_{aorta}	All	30.31 ± 11.63	39.81 ± 15.00	23.62 ± 10.11	< 0.001	0.002	< 0.001
CNR_{lesion}	All	6.02 ± 5.13	8.90 ± 7.75	5.33 ± 3.10	< 0.001	0.423	0.004
	80 kVp*	6.46 ± 4.73	9.77 ± 7.50		0.001	0.407	0.001
	100 kVp†	5.83 ± 5.36	8.53 ± 7.94		< 0.001	0.625	0.033
Image noise (HU)	All	11.10 ± 1.66	7.99 ± 1.87	9.32 ± 1.78	< 0.001	0.005	< 0.001
	80 kVp*	14.31 ± 2.69	9.56 ± 1.92		< 0.001	< 0.001	0.657
	100 kVp†	10.46 ± 2.25	7.23 ± 1.52		< 0.001	0.009	< 0.001

Data are means ± standard deviation. *Includes 8 patients with 14 lesions, †Includes 46 patients with 49 lesions. CNR = contrast-to-noise ratio, HU = Hounsfield unit

A B C

Fig. 3. Transverse contrast-enhanced CT images were obtained from 60-year-old man with hepatocellular carcinoma and cirrhosis (BMI, 23.2 kg/m^2) (A, B) with combined use of ATVS and ATCM at tube voltage of 100 kVp and from 61-year-old man with hepatocellular carcinoma and cirrhosis using ATCM alone (BMI, 20.6 kg/m^2) (C) during LAP. CNR of lesion and mean image noise in group A1 (A), group A2 (B), and group B (C) were as follows: CNR of lesion: 3.60, 4.85, and 4.01; image noise: 10.9, 7.7, and 8.0 HU. ATCM = automatic tube current modulation, ATVS = automatic tube voltage selection, BMI = body mass indices, CNR = contrast-to-noise ratio, HU = Hounsfield unit, LAP = late arterial phase

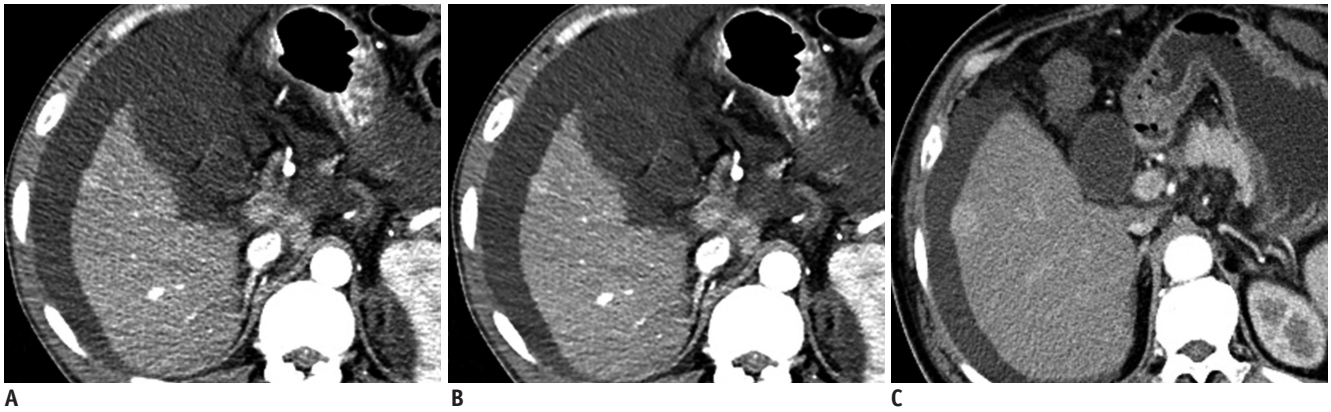

A B C

Fig. 4. Transverse contrast-enhanced CT images were obtained from 50-year-old woman with hepatocellular carcinoma and cirrhosis (BMI, 21.8 kg/m^2) (A, B) with combined use of ATVS and ATCM at tube voltage of 80 kVp and from 56-year-old woman with hepatocellular carcinoma and cirrhosis using ATCM alone (BMI, 23.4 kg/m^2) (C) during LAP. CNR of lesion and mean image noise in group A1 (A), group A2 (B), and group B (C) were as follows: CNR of lesion: 1.73, 2.61, and 2.15; image noise: 16.9, 11.9, and 9.9 HU. ATCM = automatic tube current modulation, ATVS = automatic tube voltage selection, BMI = body mass indices, CNR = contrast-to-noise ratio, HU = Hounsfield unit, LAP = late arterial phase

0.004) (Figs. 3, 4) except when compared to group A2 at 100 kVp and group B with respect to CNR_{lesion} ($p = 0.033$). The CNRs of lesions in group A2 showed no statistically significant difference ($p = 0.614$) between tube voltages of 100 kVp and 80 kVp. Compared with group B, the CNR of the aorta in group A1 was significantly higher ($p = 0.002$) and the CNRs of lesions in group A1 were not significantly different ($p > 0.05$).

Image noise in group A2 (8.0 ± 1.9 HU) was the lowest among the three groups (both $p < 0.001$), and it was decreased by 28% compared to that in group A1, and by 14% compared to that in group B. Compared with group B, image noise for group A2 was significantly lower on the 100 kVp dataset ($p < 0.001$) and it was not significantly different on the 80 kVp dataset ($p = 0.657$). Decreasing the tube voltage from 100 kVp to 80 kVp in group A2 resulted in a significant increase in image noise ($p < 0.001$). Image noise in group A1 and in group A1 scanned with the chosen 80 kVp and 100 kVp tube voltage was significantly higher than that in group B (p values ranging from < 0.001 to 0.009), and lower than that in group A2 (all p values < 0.001).

Qualitative Analysis

Results of the qualitative analysis in the three groups are shown in Table 2 and Figure 5. There was substantial

Korean Journal of Radiology
KJR

Table 2. Qualitative Analysis Results in 3 Groups

		Group A1 (57 Patients with 66 Lesions)	Group A2 (57 Patients with 66 Lesions)	Group B (48 Patients with 57 Lesions)	A1 vs. A2	A1 vs. B	A2 vs. B
Image noise	All	2.9 ± 0.6	3.9 ± 0.7	3.4 ± 0.6	< 0.001	< 0.001	< 0.001
	80 kVp*	2.4 ± 0.5	3.4 ± 0.6		< 0.001	< 0.001	0.788
	100 kVp†	3.2 ± 0.5	4.1 ± 0.6		< 0.001	0.054	< 0.001
Overall image quality	All	3.1 ± 0.5	3.6 ± 0.7	3.3 ± 0.6	< 0.001	0.062	0.022
	80 kVp*	2.8 ± 0.4	3.3 ± 0.7		0.029	0.002	0.961
	100 kVp†	3.3 ± 0.5	3.8 ± 0.6		< 0.001	0.562	0.003
Lesion conspicuity	All	3.6 ± 0.9	4.1 ± 0.8	3.4 ± 0.8	0.001	0.281	< 0.001
	80 kVp*	3.6 ± 0.8	4.2 ± 0.7		< 0.001	0.324	0.001
	100 kVp†	3.6 ± 1.0	4.1 ± 0.8		< 0.001	0.415	< 0.001

Data are means ± standard deviation. Parameters were graded on 5-point scale where image quality increases as grade increases (i.e., less noise, better overall quality, and higher conspicuity). *Includes 8 patients with 14 lesions, †Includes 46 patients with 49 lesions

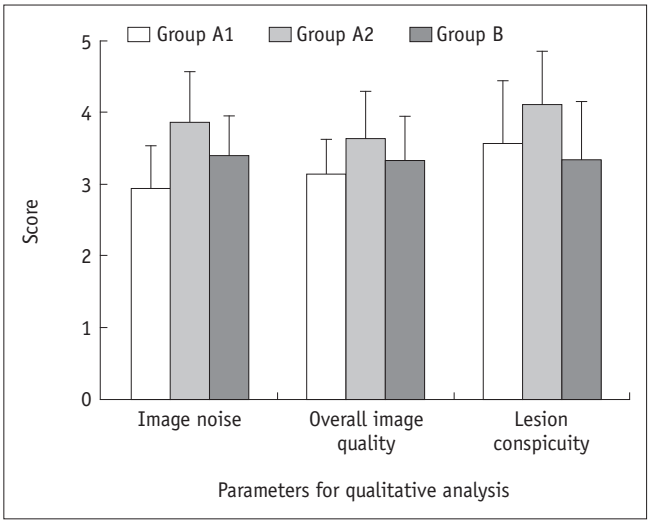

Fig. 5. Results of qualitative analysis for all lesions in terms of image noise, overall image quality, and lesion conspicuity among three groups. Group A2 showed less image noise, and higher overall image quality and lesion conspicuity than group A1 and group B (p values ranging from < 0.001 to 0.001) except for overall image quality between group A2 and group B (p = 0.022). Group B showed less image noise than group A1 (p < 0.001). There was no significant difference in overall image quality and lesion conspicuity between group A1 and group B (p > 0.05).

interobserver agreement with regard to image noise, overall image quality, and lesion conspicuity (κ = 0.75, 0.78, and 0.82, respectively).

None of the patients received an unacceptable score. All of the lesions were identifiable, with scores equal to or greater than 2. Only 2 lesions in group A1 and 5 lesions in group B scored 2. For all lesions and lesions scanned with the chosen 80 kVp and 100 kVp tube voltage, group A2 showed less image noise, and higher overall image quality and lesion conspicuity than group A1 and group B (p values ranging from < 0.001 to 0.003), except for overall image quality between group A2 at 80 kVp and group A1 (p = 0.029), between group A2 at all tube voltages and group B (p = 0.022), and between group A2 at 80 kVp and group B. Group A2 at 80 kVp scored higher in lesion conspicuity as compared with group B (p = 0.001), but displayed similar results with respect to image noise and overall image quality. Group A2 at 80 kVp had higher image noise (p = 0.001) as compared with group A2 at 100 kVp, but displayed similar lesion conspicuity (p = 0.550) and overall image quality (p = 0.051).

Group B showed less image noise than group A1 at 80 kVp, but a similar degree of image noise as that in group A1 at 100 kVp. There was no significant difference in the overall image quality and lesion conspicuity between group A1 and group B except for the overall image quality in group A1 at 80 kVp. Group A1 at 80 kVp showed lower overall image quality as compared with group B (p = 0.002).

Radiation Dose

CTDIvol, DLP, and effective radiation dose in group A (10.10 ± 5.66 mGy, 246.67 ± 131.00 mGy·cm, and 3.70 ± 1.96 mSv) were significantly lower than those in group B (12.31 ± 4.24 mGy, 304.44 ± 121.59 mGy·cm, and 4.57 ± 1.82 mSv) (p = 0.028, 0.022, 0.022, respectively). The estimated radiation dose (CTDIvol) was 23% lower for 100-kVp images (9.42 ± 2.86 mGy) and 49% lower for 80-kVp images (6.31 ± 0.48 mGy) in group A compared with that for 120-kVp images (12.31 ± 4.24 mGy) in group B (both p values < 0.001).

DISCUSSION

Our study results demonstrated that lesion conspicuity

of hypervascular liver lesions could be improved with low image noise and high overall image quality by using the combination of ATVS and ATCM with the SAFIRE algorithm. We observed an increase of 32% in CNR and a decrease of 28% in image noise compared with combined ATVS and ATCM alone, in 40% and 14% compared with ATCM alone with the standard 120 kVp tube voltage. These improvements might be due to the combined use of the higher contrast resolution at low kVp frequently recommended by ATVS (14, 17, 33) and noise reduction of the IR algorithm (34-36).

Automatic tube voltage selection recommends the tube voltage based on the attenuation detected on the patient size/scout attenuation, body region imaged, and respective indication of the CT study. In our study, 80 kVp and 100 kVp together accounted for 95% of all recommended tube voltages. The most commonly used tube voltage for all four BMI groups was 100 kVp, while 80 kVp was the most commonly used tube voltage for normal BMI and overweight patients. This result was contradictory with that of a previous study by Lee et al. (17) who reported that 80 kVp was the most frequently used tube voltage in normal BMI and underweight patients and 100 kVp was the most commonly used tube voltage in overweight patients. The difference can be partially explained by the smaller number of underweight patients (n = 2, 3.5%) and the overall small number of patients in group A (n = 57) in our study. The low correlation between BMI and recommended tube voltage demonstrated in our study might have also contributed to the results.

Generally, low tube potential images have higher contrast resolution than high tube potential images. The higher CNR of the aorta in group A1 compared to that in group B validated this notion. However, the improvement in the liver CNR was not statistically significant, which might be explained by the relatively good image quality of both image sets and small sample size. A high percentage of low tube potential images (80 kVp, 100 kVp) recommended by ATVS in group A1 displayed similar lesion CNR and lesion conspicuity compared to those on 120-kVp FBP images in group B. A possible explanation for this result might be the high image noise produced by low kVp images (19% higher compared to group B) (16, 17) and low percentage of 80 kVp (14%) recommended by ATVS. Moreover, the 100 kVp technique without the IR algorithm provided higher lesion conspicuity but without statistical significance and similar subjective image quality compared to the 120 kVp technique.

The use of SAFIRE reconstruction algorithms causes a reduction in image noise, and a simultaneous increase in the CNR (34-36). Our results are in line with those in these studies as they show a similar reduction in image noise and an improvement in CNR of lesions in group A2 at 100 kVp, and comparable image noise but improved CNR in group A2 at 80 kVp. By lowering the tube voltage from 100 kVp to 80 kVp in group A2, image noise increased significantly while CNR of hypervascular HCCs did not change significantly, which was contradictory to the results of lower sensitivity at 80 kVp compared to 100 kVp in the study of hypodense liver lesions by Husarik et al. (16). The discrepancies between these two studies can be explained by the different lesion contrasts. The lesion conspicuity depends on the radiation dose level, thereby showing that at low radiation doses, low-contrast objects cannot be detected with adequate accuracy using all reconstruction algorithms. However, high-contrast objects such as iodine-containing structures are expected to show higher signals when imaged at lower tube voltages. Although IR algorithms are somewhat beneficial in terms of lower image noise, their blotchy or plastic-like image appearance may not be acceptable to most radiologists (37). The pixelated appearance was more apparent on SAFIRE images that had high IR strengths (35, 37). In order to maintain the beneficial effect of lower image noise with SAFIRE reconstruction and to reduce the influence of pixelated appearance on SAFIRE images, SAFIRE reconstruction strength 3 was used, which caused a decrease in image noise and an increase in signal-to-noise ratio when compared with an FBP reconstruction by Baker et al. (27).

There is an exponential relationship between tube voltage and radiation dose. Lowering the tube voltage can significantly reduce the radiation dose (9, 38). Previous studies have shown that ATVS reduced the radiation dose by 39% to 55% in various simulated patient sizes (14). A radiation dose reduction of up to 31% was obtained during contrast material-enhanced liver CT (17). Overall radiation dose was reduced by 25% for body CTA, compared with the standard 120 kVp protocol (33). The combined use of ATVS and ATCM in our study resulted in a 19% decrease (23% for 100-kVp images and 49% for 80-kVp images) in the radiation dose, compared to ATCM alone using conventional 120 kVp imaging. The resulting radiation dose reduction of 23% at 100 kVp was similar to that in a previous study (28%) (16).

Our study demonstrated that the most commonly

Korean Journal of Radiology
KJR

recommended tube voltage of 100 kVp contributed more in improving lesion conspicuity and overall image quality and in decreasing the image noise than 80 kVp in the scan obtained by using the combination of ATVS and ATCM with use of the SAFIRE algorithm. This finding was consistent with the results in the study by Husarik et al. (16) who found that the combination of automatic attenuation-based tube voltage selection at 100 kVp and IR resulted in higher objective and subjective image quality and higher sensitivity for the detection of simulated hypodense liver lesions.

Our study had several limitations. This study reflects our initial experience with a small number of patients. Prospective trials are needed to validate our results. Second, there were only a limited number of patients with a BMI less than 18.5 kg/m^2 and greater than 29 kg/m^2. Additional studies are needed to validate the advantages of combined ATVS and ATCM imaging in these patients. Third, this study was limited to the two-phasic (LAP and PVP) scans, which might have missed the lesions detectable in the delayed phase. This might influence the study results. Finally, there is a limitation in generalization of the results as this study was performed using a single scanner model.

In conclusion, combined use of ATVS and ATCM and image reconstruction with SAFIRE algorithm in the scans provided higher lesion conspicuity and similar or higher subjective and objective image quality of small HCC lesions, while allowing for a radiation dose reduction of 19% compared with ATCM alone and FBP.

Acknowledgments

The authors wish to thank Dr. Fufu Chen, Dr. Xinglong Liu, and Dr. Runze Wu for their technical support in understanding the automatic tube voltage selection technology.

REFERENCES

1. Amis ES Jr, Butler PF, Applegate KE, Birnbaum SB, Brateman LF, Hevezi JM, et al. American College of Radiology white paper on radiation dose in medicine. *J Am Coll Radiol* 2007;4:272-284
2. Strzelczyk JJ, Damilakis J, Marx MV, Macura KJ. Facts and controversies about radiation exposure, part 2: low-level exposures and cancer risk. *J Am Coll Radiol* 2007;4:32-39
3. Einstein AJ, Henzlova MJ, Rajagopalan S. Estimating risk of cancer associated with radiation exposure from 64-slice computed tomography coronary angiography. *JAMA* 2007;298:317-323
4. Hall EJ, Brenner DJ. Cancer risks from diagnostic radiology. *Br J Radiol* 2008;81:362-378
5. Hall EJ, Brenner DJ. Cancer risks from diagnostic radiology: the impact of new epidemiological data. *Br J Radiol* 2012;85:e1316-e1317
6. Kramer R, Khoury HJ, Vieira JW. CALDose_X-a software tool for the assessment of organ and tissue absorbed doses, effective dose and cancer risks in diagnostic radiology. *Phys Med Biol* 2008;53:6437-6459
7. Ball CG, Correa-Gallego C, Howard TJ, Zyromski NJ, House MG, Pitt HA, et al. Radiation dose from computed tomography in patients with necrotizing pancreatitis: how much is too much? *J Gastrointest Surg* 2010;14:1529-1535
8. Smith-Bindman R, Lipson J, Marcus R, Kim KP, Mahesh M, Gould R, et al. Radiation dose associated with common computed tomography examinations and the associated lifetime attributable risk of cancer. *Arch Intern Med* 2009;169:2078-2086
9. Schindera ST, Nelson RC, Yoshizumi T, Toncheva G, Nguyen G, DeLong DM, et al. Effect of automatic tube current modulation on radiation dose and image quality for low tube voltage multidetector row CT angiography: phantom study. *Acad Radiol* 2009;16:997-1002
10. Vardhanabhuti V, Loader R, Roobottom CA. Assessment of image quality on effects of varying tube voltage and automatic tube current modulation with hybrid and pure iterative reconstruction techniques in abdominal/pelvic CT: a phantom study. *Invest Radiol* 2013;48:167-174
11. Siegel MJ, Schmidt B, Bradley D, Suess C, Hildebolt C. Radiation dose and image quality in pediatric CT: effect of technical factors and phantom size and shape. *Radiology* 2004;233:515-522
12. Tamm EP, Rong XJ, Cody DD, Ernst RD, Fitzgerald NE, Kundra V. Quality initiatives: CT radiation dose reduction: how to implement change without sacrificing diagnostic quality. *Radiographics* 2011;31:1823-1832
13. Reid J, Gamberoni J, Dong F, Davros W. Optimization of kVp and mAs for pediatric low-dose simulated abdominal CT: is it best to base parameter selection on object circumference? *AJR Am J Roentgenol* 2010;195:1015-1020
14. Schindera ST, Winklehner A, Alkadhi H, Goetti R, Fischer M, Gnannt R, et al. Effect of automatic tube voltage selection on image quality and radiation dose in abdominal CT angiography of various body sizes: a phantom study. *Clin Radiol* 2013;68:e79-e86
15. Niemann T, Henry S, Faivre JB, Yasunaga K, Bendaoud S, Simeone A, et al. Clinical evaluation of automatic tube voltage selection in chest CT angiography. *Eur Radiol* 2013;23:2643-2651
16. Husarik DB, Schindera ST, Morsbach F, Chuck N, Seifert B, Szucs-Farkas Z, et al. Combining automated attenuation-based tube voltage selection and iterative reconstruction: a liver phantom study. *Eur Radiol* 2014;24:657-667
17. Lee KH, Lee JM, Moon SK, Baek JH, Park JH, Flohr TG, et al. Attenuation-based automatic tube voltage selection and tube

current modulation for dose reduction at contrast-enhanced liver CT. *Radiology* 2012;265:437-447
18. Suh YJ, Kim YJ, Hong SR, Hong YJ, Lee HJ, Hur J, et al. Combined use of automatic tube potential selection with tube current modulation and iterative reconstruction technique in coronary CT angiography. *Radiology* 2013;269:722-729
19. Siegel MJ, Hildebolt C, Bradley D. Effects of automated kilovoltage selection technology on contrast-enhanced pediatric CT and CT angiography. *Radiology* 2013;268:538-547
20. Siegel MJ, Ramirez-Giraldo JC, Hildebolt C, Bradley D, Schmidt B. Automated low-kilovoltage selection in pediatric computed tomography angiography: phantom study evaluating effects on radiation dose and image quality. *Invest Radiol* 2013;48:584-589
21. Katsura M, Matsuda I, Akahane M, Yasaka K, Hanaoka S, Akai H, et al. Model-based iterative reconstruction technique for ultralow-dose chest CT: comparison of pulmonary nodule detectability with the adaptive statistical iterative reconstruction technique. *Invest Radiol* 2013;48:206-212
22. Gonzalez-Guindalini FD, Ferreira Botelho MP, Töre HG, Ahn RW, Gordon LI, Yaghmai V. MDCT of chest, abdomen, and pelvis using attenuation-based automated tube voltage selection in combination with iterative reconstruction: an intrapatient study of radiation dose and image quality. *AJR Am J Roentgenol* 2013;201:1075-1082
23. Korn A, Bender B, Fenchel M, Spira D, Schabel C, Thomas C, et al. Sinogram affirmed iterative reconstruction in head CT: improvement of objective and subjective image quality with concomitant radiation dose reduction. *Eur J Radiol* 2013;82:1431-1435
24. Shin HJ, Chung YE, Lee YH, Choi JY, Park MS, Kim MJ, et al. Radiation dose reduction via sinogram affirmed iterative reconstruction and automatic tube voltage modulation (CARE kV) in abdominal CT. *Korean J Radiol* 2013;14:886-893
25. Lv P, Lin XZ, Li J, Li W, Chen K. Differentiation of small hepatic hemangioma from small hepatocellular carcinoma: recently introduced spectral CT method. *Radiology* 2011;259:720-729
26. Kalra MK, Maher MM, Toth TL, Schmidt B, Westerman BL, Morgan HT, et al. Techniques and applications of automatic tube current modulation for CT. *Radiology* 2004;233:649-657
27. Baker ME, Dong F, Primak A, Obuchowski NA, Einstein D, Gandhi N, et al. Contrast-to-noise ratio and low-contrast object resolution on full- and low-dose MDCT: SAFIRE versus filtered back projection in a low-contrast object phantom and in the liver. *AJR Am J Roentgenol* 2012;199:8-18
28. WHO Expert Consultation. Appropriate body-mass index for Asian populations and its implications for policy and intervention strategies. *Lancet* 2004;363:157-163
29. Rizzo S, Kalra M, Schmidt B, Dalal T, Suess C, Flohr T, et al. Comparison of angular and combined automatic tube current modulation techniques with constant tube current CT of the abdomen and pelvis. *AJR Am J Roentgenol* 2006;186:673-679
30. Lv P, Liu J, Wu R, Hou P, Hu L, Gao J. Use of non-linear image blending with dual-energy CT improves vascular visualization in abdominal angiography. *Clin Radiol* 2014;69:e93-e99
31. Nakaura T, Awai K, Oda S, Funama Y, Harada K, Uemura S, et al. Low-kilovoltage, high-tube-current MDCT of liver in thin adults: pilot study evaluating radiation dose, image quality, and display settings. *AJR Am J Roentgenol* 2011;196:1332-1338
32. Sagara Y, Hara AK, Pavlicek W, Silva AC, Paden RG, Wu Q. Abdominal CT: comparison of low-dose CT with adaptive statistical iterative reconstruction and routine-dose CT with filtered back projection in 53 patients. *AJR Am J Roentgenol* 2010;195:713-719
33. Winklehner A, Goetti R, Baumueller S, Karlo C, Schmidt B, Raupach R, et al. Automated attenuation-based tube potential selection for thoracoabdominal computed tomography angiography: improved dose effectiveness. *Invest Radiol* 2011;46:767-773
34. Yang WJ, Yan FH, Liu B, Pang LF, Hou L, Zhang H, et al. Can sinogram-affirmed iterative (SAFIRE) reconstruction improve imaging quality on low-dose lung CT screening compared with traditional filtered back projection (FBP) reconstruction? *J Comput Assist Tomogr* 2013;37:301-305
35. Kalra MK, Woisetschläger M, Dahlström N, Singh S, Lindblom M, Choy G, et al. Radiation dose reduction with Sinogram Affirmed Iterative Reconstruction technique for abdominal computed tomography. *J Comput Assist Tomogr* 2012;36:339-346
36. Schabel C, Fenchel M, Schmidt B, Flohr TG, Wuerslin C, Thomas C, et al. Clinical evaluation and potential radiation dose reduction of the novel sinogram-affirmed iterative reconstruction technique (SAFIRE) in abdominal computed tomography angiography. *Acad Radiol* 2013;20:165-172
37. Yu MH, Lee JM, Yoon JH, Baek JH, Han JK, Choi BI, et al. Low tube voltage intermediate tube current liver MDCT: sinogram-affirmed iterative reconstruction algorithm for detection of hypervascular hepatocellular carcinoma. *AJR Am J Roentgenol* 2013;201:23-32
38. Hoang JK, Yoshizumi TT, Nguyen G, Toncheva G, Choudhury KR, Gafton AR, et al. Variation in tube voltage for adult neck MDCT: effect on radiation dose and image quality. *AJR Am J Roentgenol* 2012;198:621-627